

## SOLID OXIDE FUEL CELLS POWER UNIT REFORMER/BURNER/HEAT-EXCHANGER MODULE EXPERIMENTAL STUDY

by

**Vladimir A. MUNTS<sup>a</sup>, Yulia V. VOLKOVA<sup>a,b</sup>, Mikhail I. ERSHOV<sup>a</sup>,  
Vladimir G. TUPONOGOV<sup>a</sup>, and Nikita S. PLOTNIKOV<sup>a,b</sup>**

<sup>a</sup> Ural Federal University, Ekaterinburg, Russia

<sup>b</sup> Ural Industrial Company, Limited Liability Company, Ekaterinburg, Russia

Original scientific paper

<https://doi.org/10.2298/TSCI161105180M>

*The article contains the installation description, experimental procedure, and results for the catalytic partial oxidation reformer/catalyst burner/heat-exchanger module. Mathematical modeling for all major blocks temperatures dependence on the reformer air supply ratio was carried out. In the air supply ratio range under study the model was verified using experimental data. The model was further practically used for the solid oxide fuel cells power unit automatic control modes development. The partial oxidation reforming solid oxide fuel cells power unit characteristics were evaluated.*

**Key words:** *solid oxide fuel cells, catalytic partial oxidation reformer, experimental study, heat exchange*

### Introduction

Solid oxide fuel cells (SOFC) power units are actively developed in many countries today. These units have high efficiency up to 70% and are environmentally safe [1, 2]. Any hydrocarbon convertible into a synthesis gas can be used as fuel. Furthermore, quite high operation temperatures 750-900 °C allow these units to be implemented in hybrid SOFC-gas turbine systems [3, 4]. The research and development of the SOFC power unit with catalytic partial oxidation (CPOX) reformer is challenging as there are many blocks influencing each other's thermal conditions in the system. Therefore, its mathematical modelling for the temperatures of all major blocks and overall energy balance needs to be carried out on an experimental basis.

### Experimental procedure

To ensure the SOFC operation in the 2 kW power unit, the CPOX reformer/burner/heat-exchanger module (hereinafter the module) is used. Frequent starts and shutdowns of the module with stacks mounted in different modes can damage the SOFC stack due to the large number of thermal cycles. To have an opportunity to explore the module modes of operation and to assess their impact on the stacks of fuel cells, the module separate tests were carried out.

The synthesis gas was derived by the reaction of methane partial oxidation, eq. (1), in which  $\alpha_{\text{ref}}$  is the reformer air supply ratio is in the range from the carbon deposition boundary to 0.7 depending on the reaction temperature and natural gas composition:



\* Corresponding author, e-mail: [gibridsofc@gmail.com](mailto:gibridsofc@gmail.com)

The reaction of methane partial oxidation can be quite easily implemented in the nickel catalyst bed at temperatures of 500-900 °C.

The aim of this experimental study was to obtain the dependence of all major Module temperatures on the reformer air supply ratio and evaluate the partial oxidation reforming SOFC power unit energy characteristics.

For this study, the test facility with the Module and the cooler which was mounted instead of the fuel cells stack were used.

The test facility consisted of the following blocks, fig. 1:

- automated control system,
- gas treatment block (dust and sulfur removal, gases pressure, and flow rate maintenance),
- gas-air mixture preheating heat exchanger upstream the partial oxidation reformer,
- preheating heat exchanger for SOFC stack cathode air, and
- ring shaped natural gas partial oxidation reformer coupled with the circular catalytic burner, the same as the one used by Chang *et al.* [5] without fins in the reformer and burner.

The absence of fins is due to the fact that the reaction of eq. (1) is exothermic and there is no point in the burner-reformer heat exchange intensification.

- cooler which cools and directs the synthesis gas from the reformer to the burner for the subsequent oxidation by the cathode air, it also cools the flow in the burner as there is a high heat flux from the burner to the cooler through the metal plate, and
- exhaust gases removal block.

In the experiments, the natural gas from cylinders, which had previously been purified from sulfur compounds in the desulfurization filter with NaA zeolite, was used as fuel. The natural gas was supplied at a pressure of 0.1-0.2 MPa, which was regulated by switch panel with a reducer. After purification from sulphur compounds and dust, the natural gas

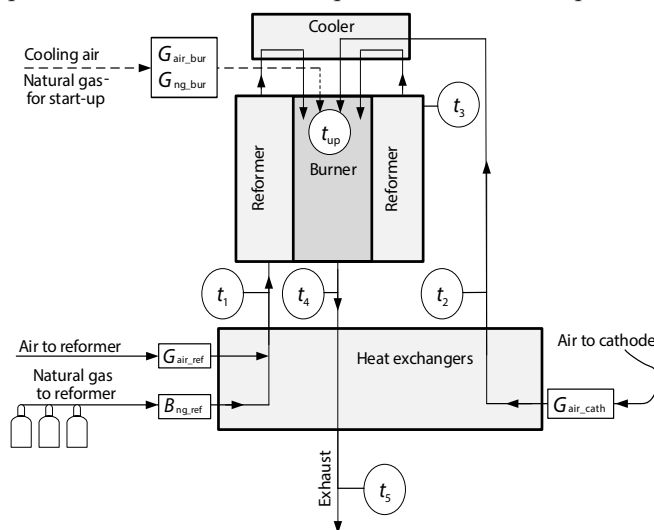


**Figure 1. The CPOX reformer/burner/heat-exchanger module and cooler test facility schematics;  $t_1, t_2, t_3, t_4, t_5$  – temperatures in the corresponding points,  $G_{air\_cath}$  – air-flow fed to the burner (coincides with the cathode air flow),  $G_{air\_ref}$  – air-flow fed to the reformer,  $B$  – natural gas-flow fed to the reformer,  $G_{air\_bur}$  – air flow additionally fed to the burner bypassing the reformer and cooler,  $G_{ng\_bur}$  – natural gas-flow fed to the burner by-passing the reformer and cooler**

was fed into the heat exchanger mixing with the filtered air. Then, the resulting gas-air mixture was heated by the burner exhaust gases and fed to the reformer. The resulting synthesis gas downstream the reformer was fed to the catalytic burner where it was combusted together with the heat exchanger pre-heated cathode air. Due to the absence of fuel cells stacks, the synthesis gas was still rich of combustible components. Therefore, it was necessary to cool the synthesis gas and the flow in the burner to reduce the burner exhaust gases temperature. The burner exhaust gases were then directed into the heat exchanger, in which they transferred heat to the gas-air mixture and cathode air.

Two series-connected blowers Domel, not shown in fig. 1, were used for the air supply, the air was fed to a receiver to reduce possible pressure pulsations. The series connection of the blowers allowed to increasing their resulting pressure. From the receiver the air with the required flow rates was fed to the three air channels: the cathode channel, the reformer path, and straight to the burner for cooling. The PID controllers were used for the air-flow regulation.

Temperature measurement was performed by Cr/Al thermocouples, a relative error of which was  $\pm 1.5\%$  when measuring temperatures up to  $375\text{ }^{\circ}\text{C}$ , and at temperatures of  $375\text{-}1000\text{ }^{\circ}\text{C}$  – the error was  $\pm 0.004\%$ . Honeywell Company industrial flow meters were used to measure air, and natural gas-flow. For air-flow in the cathode channel HAFUHT0300L4AXT model flow meter was used with a measuring range up to  $300\text{ l/min}$  and a relative precision of  $\pm 0,5\%$ . For natural gas-flow rate to the burner and reformer measurement AWM720P1 model flow meter was used with a measuring range up to  $200\text{ l/min}$  and a relative accuracy of  $\pm 0,35\%$ . Calibration of the flow meters prior to testing was performed by the volumetric method.

Supervisory control and data acquisition from the thermocouples and flow meters were organized using industrial SCADA Simplight system, data archiving was carried out with a period of 5 seconds. Continuous recording of parameters and flow rates control was displayed in the screen mnemonic diagram connected to the control system.

To reduce the wall losses the power unit casing was insulated with sheets of mineral wool, which were shielded outside with metal plates.

In accordance with the manufacturer requirements, the SOFC stacks should be heated no faster than  $1\text{-}4\text{ }^{\circ}\text{C}$  per minute, so when performing the experiments the reformer heating speed was limited.

Warming up of the reformer to the operating temperature was carried out in the following way. Initially, the natural gas at the flow rate of  $0.7\text{ l/min}$  and air at the flow rate of  $12\text{ l/min}$  were fed to the burner bypassing the reformer (excess air ratio was  $\alpha \approx 1.8$ ), after the gas-air mixture ignition in 15-20 minutes stable catalytic combustion was achieved and the flow rates were gradually increased in accordance with the required heating speed.

The nickel in the NiO was reduced to the active metal form by the flow of nitrogen and hydrogen,  $95\%\text{ N}_2/5\%\text{ H}_2$ , at an initial start-up [6].

Since there could be oxygen in the reformer at the subsequent start-up which could cause nickel reoxidation at temperatures above  $200\text{ }^{\circ}\text{C}$  [7], when the reformer temperature level reached  $100\text{ }^{\circ}\text{C}$  a mixture of shielding gases,  $95\%\text{ N}_2/5\%\text{ H}_2$ , was fed to the reformer at the flow rate of  $2\text{ l/min}$  during the whole period of start-up.

After reaching the temperature of  $t_3 = 550\text{ }^{\circ}\text{C}$  the gas-air mixture was fed to the reformer instead of the safety gases. The natural gas-flow rate was initially maintained at  $0.5\text{ l/min}$  in order to ensure the gas-air mixture proper heating in the heat exchanger and thereby avoid soot formation at the reformer entrance. The reformer air supply ratio at a temperature below  $600\text{ }^{\circ}\text{C}$  was maintained above  $0.7$ . After reaching the temperature of  $t_3 = 600\text{ }^{\circ}\text{C}$ , the burner natural gas supply valve was blocked and the burner was switched into the mode synthesis gas combustion. In the experiments, the change  $\alpha_{\text{ref}}$  was carried out by changing the amount of air in the gas-air mixture. The range of the reformer air supply ratio variation is rather small: a decrease below  $0.45$  could cause the soot formation hazard in the catalyst layer, since the reformer operation range is  $600\text{-}750\text{ }^{\circ}\text{C}$ . The increase above  $0.55$  resulted in low concentrations of combustibles in the synthesis gas. The regime was considered attained if there had been no temperature change of more than  $2\%$  within 2 hours. To determine if the thermodynamic equilibrium of reactions inside the reformer existed the synthesis gas samples were taken and analyzed with the Chromatek Crystal 5000.1 chromatograph. Absolute error of measurement for the mixture compo-

nents:  $\text{CH}_4 = 0.3\%$ ,  $\text{H}_2 = 0.23\%$ ,  $\text{CO} = 0.05\%$ ,  $\text{CO}_2 = 0.6\%$ . For the gas analysis error reduction the sample was taken two times at each point, the analysis of each sample in the chromatograph was also carried out two times. Sampling was done in each mode for all experiments.

The exhaust gases composition downstream the burner and hence the combustion completeness were monitored in real-time mode with the TESTO Term 330-2LL flue gas analyzer. Data from the TESTO Term 303 device was recorded with a period of 1 second and then automatically merged with the SCADA files. Analysis of the exhaust gases composition was carried out for the following components: CO, NO, O<sub>2</sub> (CO<sub>2</sub> – calculation using O<sub>2</sub>). Error in the measuring of O<sub>2</sub>  $\pm 0.2$  vol.%, CO  $\pm 10$  ppm (0...200 ppm), NO  $\pm 5$  ppm (0...3000 ppm).

The Module is a part of the power unit and once the SOFC stacks are mounted it can generate up to 2 kW of electricity in an automatic mode. At low SOFC fuel utilization rates the anode gas downstream the SOFC stacks combustion may overheat the catalytic burner above 1200 °C, which is dangerous for the materials used. In such situations, the additional air-flow is fed to the burner bypassing the reformer without impairing the stack operation mode to protect the catalytic burner.

When planning experiments two modes were identified according to the SOFC power unit operation which were mathematically modelled and experimentally studied:

- *Basic operating mode.* The operation, in which there are no additional flows fed to the burner bypassing the reformer (neither natural gas, nor air), the gas-air mixture is fed to the reformer according to  $\alpha_{\text{ref}}$ , the preheated cathode air is fed to the burner for the synthesis gas combustion.
- *Low power operating mode characterized by the high reformer fed natural gas-flow and low SOFC fuel utilization rates.* The operation, in which the air is fed to the burner for its cooling bypassing the reformer, the gas-air mixture is fed to the reformer according to  $\alpha_{\text{ref}}$ , the preheated cathode air is fed to the burner for the synthesis gas combustion. This mode will be short, its duration depends on how fast the system reaches the equilibrium after the natural gas-flow rate to the reformer reduction when the SOFC stacks load is decreasing.

### **Mathematical modeling of the SOFC power unit CPOX reformer/burner/heat-exchanger module**

Since the SOFC stacks should be heated to the required temperature level,  $\approx 600$  °C, before operation, one of the most important parameters is the preheated cathode air temperature  $t_2$  downstream the heat exchanger. The gas-air mixture temperature  $t_1$  downstream the heat exchanger is equally important as in case of the mixture insufficient heating the free carbon can be deposited in the lower half of the reformer damaging the equipment and impairing its operation. The reformer air supply ratio  $\alpha_{\text{ref}}$  is significant for the power unit control system as it determines the resulting synthesis gas composition and hence the SOFC voltage. With the help of mathematical modeling the influence of  $\alpha_{\text{ref}}$  on  $t_1$ ,  $t_2$ ,  $t_3$ ,  $t_4$ , and  $t_5$  temperatures was studied in order to develop the SOFC power unit automatic control system.

The module engineering mathematical model input data are: fuel type, test facility schematics, the actual design characteristics of heating surfaces, and the air- and natural gas-flow rates for each experiment.

The following standpoints and assumptions were made in the engineering model.

- The simulation basis is the equations of heat balances and heat transfer, for all elements of the system. The calculation is carried out consecutively downstream the flow of fuel, reformer and cathode channel fed air, synthesis gas, and combustion products.

- For the heat transfer calculation between the burner and reformer the empirical equations are used for Al<sub>2</sub>O<sub>3</sub> spherical particles stationary blown granular bed obtained in [8]

$$Nu = 0.17 Re^{0.79} \quad (2)$$

- For the heat transfer calculation in the heat exchangers the empirical equations are used for every flow regime and surface type according to [9, 10].
- Total losses through the thermal insulation are represented by the reformer wall losses  $Q_{wall}^{ref}$  and the cooler wall losses  $Q_{wall}^{cooler}$ . These two parameters are obtained empirically [11, 12].

The resulting conceptual engineering model consists of six equations with six variables:  $t_1$ ,  $t_2$ ,  $t_3$ ,  $t_4$ ,  $t_5$ , and  $t_{up}$ .

The first eq. (3) represents the equilibrium between the energy for the gas-air mixture heating and the heat transferred from the exhaust gases to the mixture in the heat exchanger:

$$M_{ng\_ref} [(c_{ng,t_1} t_1) - (c_{ng,t_0} t_0)] + M_{air\_ref} [(c_{air,t_1} t_1) - (c_{air,t_0} t_0)] = F_{he,ref} k_{he,ref} \Delta t_1 \quad (3)$$

The second eq. (4) allows to find the cathode air temperature downstream the heat exchanger,  $t_2$ , and represents the equilibrium between the energy for the cathode air heating and the heat transferred from the exhaust gases to the cathode air in the heat-exchanger:

$$M_{air\_cath} [(c_{air,t_2} t_2) - (c_{air,t_0} t_0)] = F_{he,cath} k_{he,cath} \Delta t_2 \quad (4)$$

The third eq. (5) is the balance between the heat received by the cathode air and gas-air mixture and the heat emitted by the exhaust gases:

$$M_{ng\_ref} [(c_{ng,t_1} t_1) - (c_{ng,t_0} t_0)] + M_{air\_ref} [(c_{air,t_1} t_1) - (c_{air,t_0} t_0)] + M_{air\_cath} [(c_{air,t_2} t_2) - (c_{air,t_0} t_0)] = M_{exh} [(c_{exh,t_4} t_4) - (c_{exh,t_5} t_5)] \quad (5)$$

The fourth eq. (6) allows to find the synthesis gas temperature downstream the reformer,  $t_3$ , taking into account the partial oxidation reaction heat in the reformer  $Q_{ref}$ , the reformer wall losses  $Q_{wall}^{ref}$  and the burner to reformer heat transfer:

$$M_{mix} [(c_{mix,t_3} t_3) - (c_{mix,t_1} t_1)] = F_{ref} k_{ref} \Delta t_{ref} + Q_{ref} - Q_{wall}^{ref} \quad (6)$$

where  $Q_{ref}$  is calculated as a function of the reformer air supply ratio using the expression from [13]:

$$Q_{ref} = \left[ \frac{(I_{CO_2} + 2I_{H_2O} - I_{CO} - 2I_{H_2}) \frac{4}{3} - 2I_{O_2}}{-\frac{1}{3}(I_{CO_2} + 2I_{H_2O} - 4I_{CO} - 8I_{H_2}) - I_{CH_4}} \right] \alpha_{ref} - \frac{M_{ng\_ref}}{\mu_{ng}} \quad (7)$$

The fifth eq. (8) allows to find the flow temperature in the upper part of the burner,  $t_{up}$ , taking into account the synthesis gas catalytic combustion, the synthesis gas and cathode air sensible heat, and the cooler insulation heat losses accounted for a high heat flux from the burner to the cooler through the metal plate:

$$M_{exh} (c_{exh,t_{up}} t_{up}) = (B_{ng\_ref} Q_{LHV}^{ng} - Q_{ref}) + Q_{phys}^{sg} + Q_{phys}^{air\_cath} - Q_{wall}^{cooler} \quad (8)$$

Due to the absence of fuel cells stacks and, thus, the synthesis gas oxidation in them, the synthesis gas combustible components concentrations are still high so as the synthesis gas combustion velocity. Therefore, its burning completes in the catalyst upper layers and the vast amount of generated heat is directed into the cooler through the metal plate. Given the catalyst upper layers are close to the burner inlet, the flow temperature in the upper part of the burner,

$t_{up}$ , can be considered significant for the burner to reformer heat transfer calculation in terms of defining the temperature difference.

The sixth eq. (9) allows to find the flow temperature downstream the burner,  $t_4$ , taking into account the burner to reformer heat transfer:

$$M_{exh} \left[ \left( c_{exh,t_{up}} t_{up} \right) - \left( c_{exh,t_4} t_4 \right) \right] = F_{ref} k_{ref} \Delta t_{ref} \quad (9)$$

Using the equations set (3)-(9) power unit operation in various modes can be modelled.

This equations set was solved using PTC Mathcad Prime 3.1 [14].

### Experimental results

The experimental data on temperatures and flow rates for all tests in the basic operation mode are shown in tab. 1. The calculated and experimental data on the synthesis gas composition for this mode are shown in tab. 2. The calculated values are represented on a dry gas basis.

**Table 1. Values  $t_2$ ,  $t_3$ ,  $t_4$ ,  $t_5$ ,  $G_{air\_cath}$ ,  $\alpha_{ref}$ , and temperature deviation from calculated values  $\Delta t$  obtained in the basic operation mode for tests 1-3**

No. test	$G_{air\_cath}$ [lmin <sup>-1</sup> ]	$\alpha_{ref}$	$t_2$ , [°C]	$\Delta t_2$ , [%]	$t_3$ , [°C]	$\Delta t_3$ , [%]	$t_4$ , [°C]	$\Delta t_4$ , [%]	$t_5$ , [°C]	$\Delta t_5$ , [%]
1	24	0.45	597.1	5.66	603.6	4.67	705.2	0.91	150.1	15.7
2	24.1	0.48	575.3	5.70	606.5	1.35	702.7	2.38	145.0	16.0
3	25.8	0.54	542.1	7.86	610.8	4.85	662.2	4.14	178.2	10.2

**Table 2. Calculated (CC) and experimental (Exp) synthesis gas composition values obtained in the basic operation mode for tests 1-3 and deviation from calculated values (Dev)**

$\alpha_{ref}$	CO <sub>2</sub> [%]			CO [%]			H <sub>2</sub> [%]			CH <sub>4</sub> [%]		
	Exp	CC	Dev	Exp	CC	Dev	Exp	CC	Dev	Exp	CC	Dev
0.45	5.35	7.0	23.6	10.1	7.5	34.7	24.2	21.4	13.1	0.56	1.67	66.5
0.48	4.40	7.3	39.7	10.3	6.9	49.3	23.9	20.3	17.7	0.44	1.25	64.8
0.54	6.16	8.0	23.0	6.00	5.6	7.14	17.3	17.8	2.81	0.33	0.74	55.4

### Results and discussion

Analysis of the synthesis gas composition on the components balance basis shows that carbon deposition takes place in tests 1 and 2. The calculated carbon deposition for the temperature of 600 °C is equal to 0.42, which is close enough to the actual  $\alpha_{ref}$  values in tests 1 and 2. As the temperature gradient is present in the reformer catalyst bed, the flow temperature near the reformer outer wall is obviously lower than the average flow temperature in the same reformer cross-section which causes the soot formation by the reaction:  $2CO = C + CO_2$ . The same carbon deposition zone encounter is described in the article [15, 16]. In addition, the calculated methane concentration is almost twice as high as the actual one for all tests which is accounted for the fact that the reformer inlet temperature is at the level of 680-700 °C, therefore a greater amount of methane reacted.

To evaluate the feasibility of the proposed engineering model the calculation results were compared with the experimental data obtained in the basic operating mode.

While modeling for all major blocks temperatures dependence on the reformer air supply ratio  $\alpha_{ref}$  the following parameters were used:

- the cathode air-, and natural gas-flow rates in tests 1-3 held almost constant, tab. 1; therefore, the average values of these parameters were used, namely  $G_{air\_cath} = 24.63$  [L/min],  $B_{ng\_ref} = 2.17$  [L/min], and
- the reformer air supply ratio  $\alpha_{ref}$  changed from 0.4 to 0.55 in increments of 0.01 during calculation.

From the fig. 2 it is evident that the calculated values correlate well with the experimental ones for tests 1 and 2, tab. 1. As for the test 3 where  $\alpha_{ref} = 0.54$ , the deviation of results is greater and is probably accounted for the soot formation in tests 1 and 2 due to the operation at the carbon deposition boundary which has affected the synthesis gas compositions in these tests and the CO concentration increased. All temperatures of the module except the synthesis gas temperature downstream the reformer decrease with rising air supply ratio  $\alpha_{ref}$ . It is accounted for increasing the amount of oxygen reacted with the natural gas and heat generation in the reformer and, hence, decreasing the amount of combustibles in the synthesis gas [17]. Besides, since the natural gas and cathode air-flow rates remain constant the reformer fed air-flow rate increases so as the burner exhaust gases mass-flow rate.

The engineering model allows to calculate quite well all the module temperatures dependence on the reformer air supply ratio for the given experiments enabling us to recommend it for automatic control programs development and the power unit operation analysis.

### The SOFC power unit characteristics evaluation (the module and two SOFC stacks)

To assess the partial oxidation reforming SOFC power unit characteristics with the module described in the section *Experimental procedure* and SOFC stacks, consist of planar cells, the calculations were made on the basis of the experiment and data provided by the manufacturer of the SOFC stacks (SOFCMAN, China). The stacks contain elements with dimensions of  $0.15 \times 0.15$  m, with a supporting anode of Ni-YSZ. The stack temperature operational range is 700-800 °C, current operational range 0-27.5 A, minimum cell voltage OCV (open circuit voltage) is 0.7 V, the minimum SOFC stack voltage is 28 V, [18]. The synthesis gas was derived from methane under the following conditions: partial oxidation with air according to reaction of eq. (1), the reforming temperature was 700 °C, the nickel based catalyst was used  $\alpha_{ref} = 0.4 - 0.5$ . The methane-flow rate was maintained at 4 L/min. The experimental V-I curve of a single SOFC stack is given in fig. 3. The SOFC fuel utilization rate at the current of 20 A for a single stack was 58%, and gross power efficiency  $\eta = N_{electric} / (B_{ref} Q_{LHV}) = 19\%$ . The single cell voltage decreased from 0.89-0.56 V with increasing the current. From the V-I curve, fig. 3, the average resistance (*AR*) of the stack at different currents was obtained using the linearization method, fig. 4, [19, 20]. The figure shows that at currents of up to 2.5 A the *AR* is quite

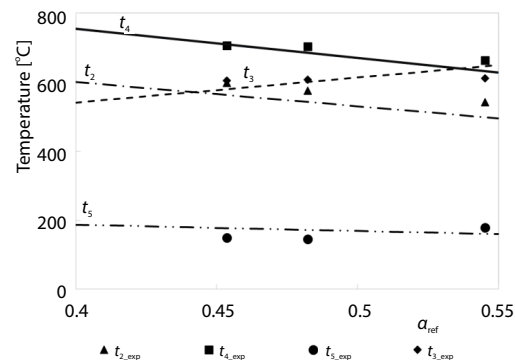


Figure 2. Modeled values of  $t_2, t_3, t_5, t_4$  vs.  $\alpha_{ref}$  according to the eqs. set (3)-(9) (lines), experimental values of  $t_2$  (▲),  $t_3$  (◆),  $t_4$  (■),  $t_5$  (●) for the basic operating mode

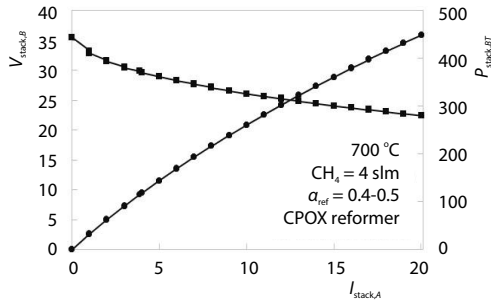


Figure 3. Partial oxidation reforming SOFC stack current-voltage characteristic

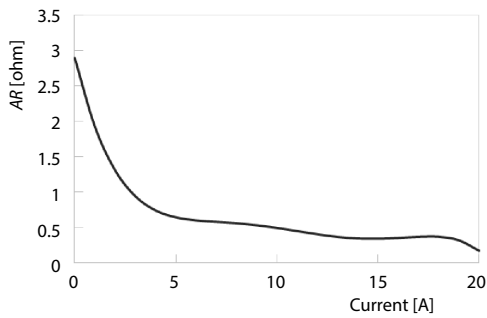


Figure 4. Partial oxidation reforming SOFC stack average resistance dependence on current

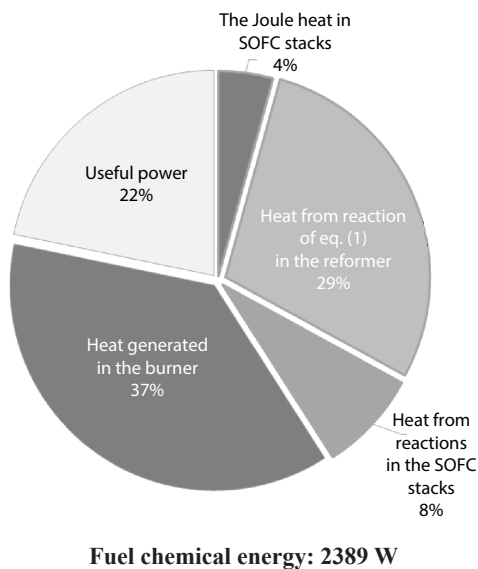


Figure 5. Partial oxidation reforming SOFC power unit fuel chemical energy consumption (module and two SOFC stacks)

high which is accounted for the activation losses while in the range from 5-20 A the resistance is approximately 0.5 ohm.

The following conditions were used for the SOFC power unit characteristics evaluation:

- number of the SOFC stacks in the hot box: 2 pcs,
- stacks electrical connection: series,
- single SOFC stack current is 10 A,
- the methane-flow rate is 4 L/min,
- reformer air supply ratio  $\alpha_{ref} = 0,45$ ,
- fuel utilization rate is 63%, and
- power output is 520 W.

For these conditions the power unit of two SOFC stacks and module efficiency is 22%. Obviously, the total losses through the thermal insulation will be significant, because in Module two exothermic reactions are coupled in contrast to the units with steam reforming, where exothermic and endothermic reactions are coupled. Figure 5 depicts a diagram, which shows that 66% of fuel chemical energy will be turned into heat in the reformer and burner, which is accounted for the relatively moderate fuel utilization rate and air supply ratio  $\alpha_{ref}$ , used in simulation. The rest amount of heat, 293 W, is generated in the stacks as the cell reaction enthalpy change and Joule heat. The remaining fuel chemical energy is used in the form of electricity by a load.

## Conclusions

- The module tests indicate its feasibility in all operating modes albeit the short-term soot formation. The synthesis gas composition downstream the reformer is almost equal to the thermodynamically-equilibrium one.
- The created engineering model allows to decently simulate the module heat exchange processes for given inlet flow rates which can be used for the new SOFC power units design and their automatic control programs development.
- The module temperatures dependence on the reformer air supply ratio was studied. All temperatures of the module  $t_1, t_2, t_4, t_5$  but for the synthesis gas temperature downstream the reformer  $t_3$  decrease with rising air supply ratio  $\alpha_{ref}$  from 0.4-0.55. It is accounted for the re-

former heat generation and the exhaust gases mass-flow rate increase and the burner heat generation decrease.

- The SOFC power unit of two stacks and the module characteristics were evaluated for the current of 10 A and the methane-flow rate of 4 L/min.

## Nomenclature

$AR$  – average resistance, [ohm]  
 $c$  – specific heat per unit mass, [ $\text{Jkg}^{-1}\text{K}^{-1}$ ]  
 $d$  – diameter, [m]  
 $F_{\text{he,cath}}$  – cathode air preheating heat exchanger tubes outer surface area, ( $= n_h n_{\text{he,cath}} \pi d_{\text{ext}} L$ ), [ $\text{m}^2$ ]  
 $F_{\text{he,ref}}$  – gas-air mixture preheating heat exchanger tubes outer surface area, ( $= n_h n_{\text{he,ng}} \pi d_{\text{ext}} L$ ), [ $\text{m}^2$ ]  
 $F_{\text{ref}}$  – reformer inner tube outer surface area, [ $\text{m}^2$ ]  
 $I$  – enthalpy, [ $\text{Jmol}^{-1}$ ]  
 $k_{\text{he,cath}}$  – exhaust gases to cathode air heat transfer coefficient in the cathode air preheating heat exchanger, [ $= 1 / (1 / \alpha_{\text{cath}} + 1 / \alpha_{\text{exh}})$ ], [ $\text{Wm}^{-2}\text{K}^{-1}$ ]  
 $k_{\text{he,ref}}$  – exhaust gases to gas-air mixture heat transfer coefficient in the gas-air mixture preheating heat exchanger, [ $= 1 / (1 / \alpha_{\text{mix}} + 1 / \alpha_{\text{exh}})$ ], [ $\text{Wm}^{-2}\text{K}^{-1}$ ]  
 $k_{\text{ref}}$  – burner to reformer heat transfer coefficient, [ $\text{Wm}^{-2}\text{K}^{-1}$ ]  
 $L$  – tube length, [m]  
 $M_{\text{air,cath}}$  – cathode air mass-flow rate, ( $= G_{\text{air,cath}} \rho_{\text{air}}$ ), [ $\text{kgs}^{-1}$ ]  
 $M_{\text{air,ref}}$  – mass-flow rate upstream the reformer, ( $= G_{\text{air,ref}} \rho_{\text{air}}$ ), [ $\text{kgs}^{-1}$ ]  
 $M_{\text{exh}}$  – exhaust gases mass-flow rate, ( $= M_{\text{ng,ref}} + M_{\text{air,ref}} + M_{\text{air,cath}}$ ), [ $\text{kgs}^{-1}$ ]  
 $M_{\text{mix}}$  – gas-air mixture mass-flow rate upstream the reformer, ( $= M_{\text{ng,ref}} + M_{\text{air,ref}}$ ), [ $\text{kgs}^{-1}$ ]  
 $M_{\text{ng,ref}}$  – natural gas mass-flow rate upstream the reformer, ( $= B_{\text{ng,ref}} \rho_{\text{ng}}$ ), [ $\text{kgs}^{-1}$ ]  
 $M_{\text{ox}}$  – actual amount of oxidizer, [mol]  
 $M_{\text{ox}}^{\text{st}}$  – amount of oxidizer stoichiometrically required for complete oxidation, [mol];  
 $N_{\text{electric}}$  – net power output, [W]  
 $\text{Nu}$  – Nusselt number ( $= \alpha \delta / \kappa$ ), [-]  
 $n$  – number of tubes [-]  
 $Q$  – heat flux (sensible heat, heat losses, reaction heat), [W]  
 $Q_{\text{LHV}}^{\text{ng}}$  – natural gas low heating value (the only exception for  $Q$ ), [ $\text{Jm}^{-3}$ ]  
 $Q_{\text{phys}}^{\text{air-cath}}$  – cathode air sensible heat upstream the burner, ( $= M_{\text{air,cath}} c_{\text{air}} t_2$ ), [W]  
 $Q_{\text{phys}}^{\text{sg}}$  – synthesis gas sensible heat upstream the burner, ( $= M_{\text{mix}} c_{\text{sg}} t_3$ ), [W]  
 $\text{Re}$  – Reynolds number ( $= v \delta / \nu$ ), [-]

$t$  – temperature, [ $^{\circ}\text{C}$ ]  
 $\Delta t_1$  – gas-air mixture preheating heat exchanger logarithmic mean temperature difference, ( $= [(t_5 - t_0) - (t_4 - t_1)] / [\ln(t_5 - t_0) / (t_4 - t_1)]$ ), [ $^{\circ}\text{C}$ ]  
 $\Delta t_2$  – cathode air preheating heat exchanger logarithmic mean temperature difference, ( $= [(t_5 - t_0) - (t_4 - t_2)] / [\ln(t_5 - t_0) / (t_4 - t_2)]$ ), [ $^{\circ}\text{C}$ ]  
 $\Delta t_{\text{ref}}$  – coupled reactor (burner and reformer) logarithmic mean temperature difference, ( $= [(t_{\text{up}} - t_3) - (t_4 - t_1)] / [\ln(t_{\text{up}} - t_3) / (t_4 - t_1)]$ ), [ $^{\circ}\text{C}$ ]

## Greek symbols

$\alpha$  – surface heat exchange coefficient, [ $\text{Wm}^{-2}\text{K}^{-1}$ ]  
 $\alpha_{\text{ref}}$  – reformer air supply ratio (the only exception for  $\alpha$ ), ( $= M_{\text{ox}} / M_{\text{ox}}^{\text{st}}$ ), [-]  
 $\delta$  – characteristic dimension, [m]  
 $\kappa$  – fluid thermal conductivity, [ $\text{Wm}^{-1}\text{K}^{-1}$ ]  
 $\mu_{\text{ng}}$  – natural gas molar mass, [ $\text{kgmol}^{-1}$ ]  
 $\nu$  – fluid kinematic viscosity, [ $\text{m}^2\text{s}^{-1}$ ]  
 $\rho$  – density, [ $\text{kgm}^{-3}$ ]  
 $v$  – flow speed, [ $\text{ms}^{-1}$ ]

## Subscripts and superscripts

air – air  
 cath – cathode flow  
 cooler – module cooler  
 electric – power unit electric part  
 exh – exhaust gases  
 h – heightwise  
 he – heat exchanger  
 mix – gas-air mixture  
 ng – natural gas  
 ox – oxidizer  
 phys – sensible (heat)  
 ref – reformer  
 sg – synthesis gas  
 wall – losses through the wall  
 0 – ambient parameter  
 1, 2, 3, 4, 5, up – module flows as per fig 1.

## Acronym

LHV – low heating value

## References

- [1] Park, J., et al., *Introduction to Thermodynamics: Transferring Energy from Here to There*, Coursera, University of Michigan, Ann Arbor, Mich., USA
- [2] Malekbala, M. R., et al., Modeling and Control of Proton Exchange Membrane Fuel Cell with Air Compressor According to Requested Electrical Current, *Thermal Science*, 19 (2015), 6, pp. 2065-2078
- [3] Henke, M., et al., Operational Aspects for Direct Coupling of Gas Turbine and Solid Oxide Fuel Cells, *ECS Transactions*, 68 (2015), 1, pp. 79-84
- [4] Pierobon, L., et al., Thermodynamic Analysis of an Integrated Gasification Solid Oxide Fuel Cell Plant Combined with an Organic Rankine Cycle, *Renewable Energy*, 60 (2013), Dec., pp. 226-234
- [5] Chang, T. G., et al., An Experimental Study on the Reaction Characteristics of a Coupled Reactor with a Catalytic Combustor and a Steam Reformer for SOFC Systems, *International Journal of Hydrogen Energy*, 37, (2012), 4, pp. 3234-3241
- [6] Halinen, M., et al., Experimental Study of SOFC System Heat-Up without Safety Gases, *International Journal of Hydrogen Energy*, 39 (2014), 1-2, pp. 552-561
- [7] Heddrich, M. P., et al., Thermodynamic Influence Analysis of Available Fuels and Reforming Methods on SOFC System Efficiency, *ECS Transaction*, 35 (2011), 1, pp. 955-962
- [8] Thiagalingam, I., et al., Exact Non Local Expression for the Wall Heat Transfer Coefficient in Tubular Catalytic Reactors, *International Journal of Heat and Fluid Flow*, 54 (2015), Aug., pp. 97-106
- [9] Liu, S., Sakr, M., A Comprehensive Review on Passive Heat Transfer Enhancements in Pipe Exchangers, *Renewable and Sustainable Energy Reviews*, 19 (2013), Mar., pp. 64-81
- [10] Jedsadaratanachai, W., et al., 3-D Numerical Study on Flow Structure and Heat Transfer in a Circular Tube with V-Baffles, *Chinese Journal of Chemical Engineering*, 23 (2015), 2, pp. 342-349
- [11] Chen, W. L., Yang, Y. C., An Iterative Regularization Method in Estimating the Transient Heat-Transfer Rate on the Surface of the Insulation Layer of a Double Circular Pipe, *Energy Conversion and Management*, 50, (2009), 12, pp. 3096-3103
- [12] Kecebas, A., Determination of Insulation Thickness by Means of Exergy Analysis in Pipe Insulation, *Energy Conversion and Management*, 58 (2012), Jun., pp. 76-83
- [13] Baskakov, A., et al., The Calculation of the Auto-Thermal, Mode of Operation of Solid Oxide Fuel Cells with Air Reformer, (in Russian), *Jenergetika Tatarstana*, 38 (2015), 2, pp. 47-51
- [14] \*\*\*, PTC Company site, <http://ru.ptc.com/product>, relevance April 04, 2015
- [15] Baskakov, A., et al., Assessment of Possibilities for Operation of Ni-Catalyst Partial Oxidation Reformers in SOFC Systems after Soot Formation, *ECS Transactions*, 68 (2015), 1, pp. 327-332
- [16] Velasco, J. A., et al., Synthesis Gas Production for GTL Applications: Thermodynamic Equilibrium Approach and Potential for Carbon Formation in a Catalytic Partial Oxidation Pre-Reformer, *Journal of Natural Gas Science and Engineering*, 20 (2014), Sept., pp. 175-183
- [17] Yan, Y., et al., Properties of Thermodynamic Equilibrium-Based Methane Autothermal Reforming to Generate Hydrogen, *International Journal of Hydrogen Energy*, 38 (2013), 35, pp. 15744-15750
- [18] Munts, V. A., et al., Studying the Characteristics of a 5 kW Power Installation on Solid Oxide Fuel Cells with Steam Reforming of Natural Gas, *Thermal Engineering*, 62 (2015), 11, pp. 779-784
- [19] Camblong, H., et al., Design of a SOFC/GT/SCs Hybrid Power System to Supply a Rural Isolated Microgrid, *Energy Conversion and Management*, 117 (2016), Jun., pp. 12-20
- [20] Aydin, O., et al., Reliability of the Numerical SOFC Models for Estimating the Spatial Current and Temperature Variations, *International Journal of Hydrogen Energy*, 41 (2016), 34, pp. 15311-15324